2013-07-16

Atypical P-type ATPases, CtpE and CtpF from Mycobacteria tuberculosis

Evren Kocabas
Worcester Polytechnic Institute

Follow this and additional works at: https://digitalcommons.wpi.edu/etd-theses

Atypical P-type ATPases, CtpE and CtpF from

Mycobacteria tuberculosis

by

Evren Kocabaş

A Thesis

Submitted to the Faculty of the

WORCESTER POLYTECHNIC INSTITUTE

in partial fulfillment of the requirements for the

Degree of Master of Science

In Biochemistry

_____

October 2013

APPROVED:

_____

Dr. José Argüello, Major Advisor

_____

Dr. Arne Gericke, Head of Department

ABSTRACT

Mycobacterium tuberculosis causes tuberculosis, one of the most life-threatening diseases of all time. It infects the host macrophages and survives in its phagosome. The host phagosome is a very hostile environment where *M. tuberculosis* copes with high concentration of transition metals (Zn^{2+}, Cu^{2+}), low levels of others (Mn^{2+}, Fe^{2+}) and acidic pH. P-ATPases are membrane proteins that transport various ions against their electrochemical gradients utilizing the energy of ATP hydrolysis. Based on their primary sequences; seven of the twelve mycobacterial ATPases are classified as putative heavy metal transporters and a K+-ATPase, while the substrate of four (CtpE, CtpF, CtpH and CtpI) remains unknown. Consistent with their membrane topology and conserved amino acids, CtpE and CtpF are possibly P2 or P3-ATPases that transport alkali metals or protons. We examined the cellular roles of orthologous CtpE and CtpF in *M. smegmatis*, a non-pathogenic model organism. We hypothesized that these novel P- ATPases play an important role in transporting alkali metals and/or protons. We analyzed growth fitness of strains carrying mutations of the coding gens of these enzymes, in presence of various metals and different pHs, as well as the gene expression levels under different stress conditions. We observed that the *M. smegmatis* mutant strains, lacking of CtpF or CtpE, are sensitive to high concentrations (mM) of Mn^{2+}. Furthermore, CtpE mutant is sensitive to alkali pH. Our results indicate that CtpE and CtpF might be an Mn^{2+} or H^+-ATPase that are required for cell's homeostasis sustainability.

ACKNOWLEDGEMENTS

TABLE OF CONTENTS

LIST OF FIGURES AND TABLES

1 INTRODUCTION

According to recent World Health Organization (WHO) studies, more than one-third of the world's population is infected with *Mycobacterium tuberculosis*, the pathogen that causes tuberculosis. P-type ATPases are membrane proteins that transport a variety of monovalent and divalent metals across biological membranes utilizing the energy produced by ATP hydrolysis. [1] Genomic analyses revealed that *M. tuberculosis* has a diverse group of metal transporters, mostly P-ATPases. [2] The abundance of these transporters might be crucial for mycobacterial survival in the host. Our focus was to identify the functional roles of putative P-ATPases, CtpE, CtpF, CtpH and CtpI in *M. tuberculosis*.

1.1 Metals in Bacteria

1.1.1 Transition metals in bacteria

Transition metals such as (Cu^+, Zn^{2+}, Fe^{2+}, Co^{2+}, Ni^{2+} and Mn^{2+}) are essential micronutrients to all life forms because of their unique chemical and physical properties. They participate in diverse biochemical pathways ranging from cellular respiration to gene expression. These metals are necessary for structural stability or catalytic activity of proteins. For instance, they constitute enzyme active sites, stabilize enzyme geometry structure, form weak-bonds with substrates, and stabilize charged transition states. Deficiencies in intracellular metal homeostasis lead to toxicity by forming oxygen radicals or mismatching the metal cofactor required for a metalloenzymes optimal functionality. [3-5] Transmembrane transporters, chaperones, storage molecules and metal-responsive transcriptional regulators maintain the homeostasis of transition metals in the cell. Besides, transition metals are associated with bacterial

virulence and host defense. The host defense system eliminates a pathogen in its macrophages by either accumulating or dispersing metals, among other chemical insults. [6] Wagner *et al.* [7] detected $Cu^{+/2+}$ accumulation in the phagosome of macrophages that contained *Mycobacterium avium*. Similarly, *M. tuberculosis* encounters harsh environmental conditions in macrophages such as low pH, high concentrations of some transition metals (Zn^{2+}, Cu^{2+}) and low levels of others (Ca^{2+}, Mn^{2+}, Fe^{2+}). [8] An important role of metals in virulence also is closely related to the presence of free oxygen and nitrogen radicals that the host immune system produces to eliminate infections. For example, macrophages will initiate the production of these free radicals to damage the endocyted pathogen. [9] Mn^{2+} is a vital transition metal and one of the relevant transition metal ions for our study. It is an essential component of many free-radical detoxifying proteins such as catalases, superoxide dismutases, or peroxidases. [10] For example, superoxide dismutase (SodA) is an Mn^{2+}-cofactored enzyme and contributes to the detoxification of superoxide in bacteria and archea. [11] A study showed that the H_2O_2 sensor element (OxyR) in *Escherichia coli* activates the import of Mn^{2+}. [12] Mn^{2+} also plays an important role in virulence and pathogenesis of several human microbial pathogens. [10, 13] For instance, CtpC, an essential Mn^{2+} P-ATPase for *M. tuberculosis*'s survival in the host*,* can maintain Mn^{2+} homeostasis, and reduce redox stress. [14] All sequenced bacterial genomes contain either one or two major classes of manganese transporters that are NRAMP (Natural-Resistance-Associated Macrophage Protein) and Mn^{2+}-permeases [10]; however, few bacterial species such as *Lactobacillus plantarum, M. tuberculosis, and M. smegmatis* have a third class of Mn^{2+} transporters like P-ATPases. [14, 15] Mn^{2+} transporters can translocate other metals. In eukaryotes, Secretory Pathway Ca^{2+}-ATPase (SPCA) not only transports Mn^{2+}, but also transports Ca^{2+} [10], while the mycobacterial Mn^{2+} transporter, NRAMP transports Fe^{2+} and Zn^{2+}. [11] The physiological roles of Mn^{2+} in *M. tuberculosis* is not well understood; however, it has been shown that Mn^{2+}-dependent enzymes contribute in metabolic functions especially free radical detoxification, central carbon metabolism, signal transduction and growth regulation. [11]

1.1.2 Alkali earth metals in bacteria

Alkali earth metals belong to Group 2A of the periodic table, including calcium which is essential to all living organisms. Ca^{2+} plays a major role in the regulation of diverse bacterial processes such as chemotaxis, cell division, and maintenance of cell structure. [16] In eukaryotic responses to environmental changes, Ca^{2+} functions as a second messenger for external signals to elicit a downstream cascade of events that result in an instantaneous change in intracellular free-Ca^{2+} concentration, $[Ca^{2+}]_i$.[16] Similarly, in bacteria Ca^{2+} also acts as an intracellular messenger through primary (P-type Ca^{2+}-ATPase) and secondary (Ca^{2+} - H^+ antiporter) transporters, and Ca^{2+} channels. [16-20] Although the transport mechanism of Ca^{2+} in bacteria has not been clarified yet; at the structural level, prokaryotic Ca^{2+}-ATPases and ion channels have remarkable similarities with their eukaryotic analogues. [19, 20] For instance, the P-type Ca^{2+}-ATPase from *Bacillus subtilis* shares 9 out of 10 critically conserved calcium binding residues with its eukaryotic counterpart, the endo(sarco)plasmic reticulum (SERCA) Ca^{2+} transporters. [19] Mycobacterial infection stimulates an increase in cytosolic Ca^{2+} concentration of macrophages to activate the phagocyte respiratory burst, production of nitric oxide and synthesis of proinflammatory mediators. [21] *M. tuberculosis* requires low cytosolic Ca^{2+} to infect human macrophages because high cytosolic Ca^{2+} concentration inhibits the phagosome–lysosome fusion and intracellular viability. [22] Thereby, Ca^{2+} transport in mycobacteria is likely associated with intracellular pathogenesis of tuberculosis.

1.2 pH regulation in bacteria

All organisms have to maintain a certain value of internal pH (cytoplasmic pH or $(pH)_i$) for their survival according to their habitat. Most bacteria inhabit wide-range of external pH values, from 5.5 to 9.0, and sustain their $(pH)_i$ values within the narrow range of pH 7.4-7.8. [23] Thus, bacterial pH homeostatic systems are able to acidify or alkalinize the cytoplasm responding to the external *milieu,* and maintain their $(pH)_i$ neutral. The regulation of pH homeostasis in bacteria is maintained by two homeostatic systems, active and passive. The active system depends on the movement of K^+, Na^+ and H^+ cations through the cell membrane by Na^+(or K^+) -H^+ antiporters, while the passive system is linked to the proton impermeability of the membrane, such as its lipid composition and the buffering capacity of the cytoplasm. [24] For example, pH homeostasis in *E. coli* is achieved by the K^+ efflux systems, KefB and KefC, and is tightly linked with glutathione-dependent detoxification mechanisms. [24] By the nature of its habitat, mycobacteria generally cope with both acidic and mildly acidic pH. For instance, saprophytic mycobacteria are able to live in acidic conditions (pH 3.5-4.3) in soil and aquatic habitats. [25] *M. tuberculosis* and *M. bovis* can survive in the phagocytic vacuole of host macrophages where the pH is mildly acidic (pH 6). [26-28] Similar to *M. tuberculosis, M. smegmatis* is able to tolerate and live in acidic conditions such as pH 5·0. [29] Although a study showed that cytoplasmic membrane permeability to H^+ ions and H^+ efflux by the F_1F_0-ATPase are two critical elements for sustaining *M. smegmatis* and *M. bovis'* cytoplasmic pH close to neutral, the mechanism of $(pH)_i$ regulation in mycobacteria is still unclear. [28]

1.3 Mycobacterial survival in Macrophages and Virulence

Macrophages are the key component of host defense against intracellular pathogens such as *M. tuberculosis*. The success of mycobacterium species as pathogens depends on their ability to maintain an infection inside the phagocytic vacuole of the macrophage. To survive within macrophages, *M. tuberculosis* inhibits the transformation of phagosomes into fully bactericidal phagolysosomes. [30] *M. tuberculosis* is able to infect the host for months to years and survive host's activated immune system. This suggests that *M. tuberculosis* is capable of adapting to continuous change of host environment such as low pH, high concentrations of some transition metals (Zn^{2+}, Cu^{2+}) and low levels of Mn^{2+}, Fe^{2+}. [8] [7, 31, 32] Hence, mycobacteria have unique pathogenic abilities, however; the mechanism of its intraphagosomal survival remains still unclear. [33]

1.4 P-type ATPases

For organisms, it is vital to control and maintain physiological concentrations of essential intracellular micronutrients such as metals because the excessive amount of them is toxic to the cell. Metal homeostasis is defined as sustainability of an optimal metal concentration, regulation of metal uptake and intracellular trafficking with efflux/storage processes. The metal requirements must be provided for the cell survival; therefore, the efflux of excessive amounts of metal ions such as Co^{2+}, Cu^{2+} and Zn^{2+} are critically important for heavy metal contamination of an organisms' habitat. [34, 35 36] In bacteria, metal homeostasis is mainly sustained by membrane transport systems such as ATP-binding cassette

(ABC) and P-ATPases, which are driven by the hydrolysis of ATP on the cytoplasmic side of the membrane, NRAMPs, or cation diffusion facilitator (CDF) proteins that are coupled to an energetically favorable transfer of protons or other ions across the bilayer. [37]

The first P-type ATPases were described as Na^+, K^+-stimulated protein that hydrolyzed Adenosine triphosphate (ATP) to transport Na^+ and K^+ ions across the axonal membrane and generated membrane potential in crab nerve cells. [38] Later on, other P-ATPases with similar characteristics were found in various tissues and organisms. Now, P-ATPases are defined as membrane proteins that transport a variety of monovalent and divalent metals across biological membranes utilizing the energy produced by ATP hydrolysis including K^+, Na^+, H^+, Ca^{2+}, Mg^{2+}, Cu^{2+}, Cd^{2+}, Zn^{2+} and phospholipids. [1]

Phylogenetic analysis from completed sequences of bacteria, archea, and eukaryote indicates that P-ATPases constitute a large superfamily. According to proposed topological arrangements and ion specificity based on their primary protein sequences they are classified into five subclasses. [39, 40]

All P-ATPases share similar structure, which consists of multiple domains with a molecular mass between 70-150 kDa that includes a cytoplasmic side with carboxyl and amino ends, and large transmembrane segments (TM) (Figure 1). Structurally and functionally, all P-ATPases share the following four major domains: the membrane (TM), actuator (A), phosphorylation (P), and nucleotide binding (N) domains. Characteristics for P-ATPases include the insertion of 10 hydrophobic transmembrane segments (TM1-TM10) (some have only six or

eight) and highly conserved cytoplasmic domains between helices TM2 and TM3, and between TM4 and TM5. For instance, DKTGTLT sequence is a highly conserved motif in the P-domain, where Asp residue is reversibly phosphorylated (Figure 1). The number of transmembrane segments in P-ATPases is correlated to the probability of being a certain type of ion transporter. [40] Based on sequence homology, P-ATPases are classified in 5 major branches, types 1-5, and partitioned into a total of 11 subclasses, 1A, 1B, 2A–2D, 3A, 3B, 4, 5. [39] P_{1A}-ATPases are involved in bacterial K^+ transport systems, P_{1B}-ATPases are heavy-metal pumps, P_{2A}-ATPases and P_{2B}-ATPases are Ca^{2+} pumps, P_{2C}-ATPases are Na^+-K^+ and H^+-K^+ pumps in animals, P_{2D}-ATPases are Na^+ pumps in fungi, P_{3A}-ATPases are plasma membrane H^+ pumps, and P_4-ATPases are putative lipid flippases. The substrate specificity of P_5-ATPase pumps has not been determined yet (Table 1). [41] Based on their membrane topology, *M. tuberculosis* CtpE, CtpF, CtpH and CtpI proteins are similar to P_2 or P_3-ATPases. Therefore, our study will focus on the proteins' features.
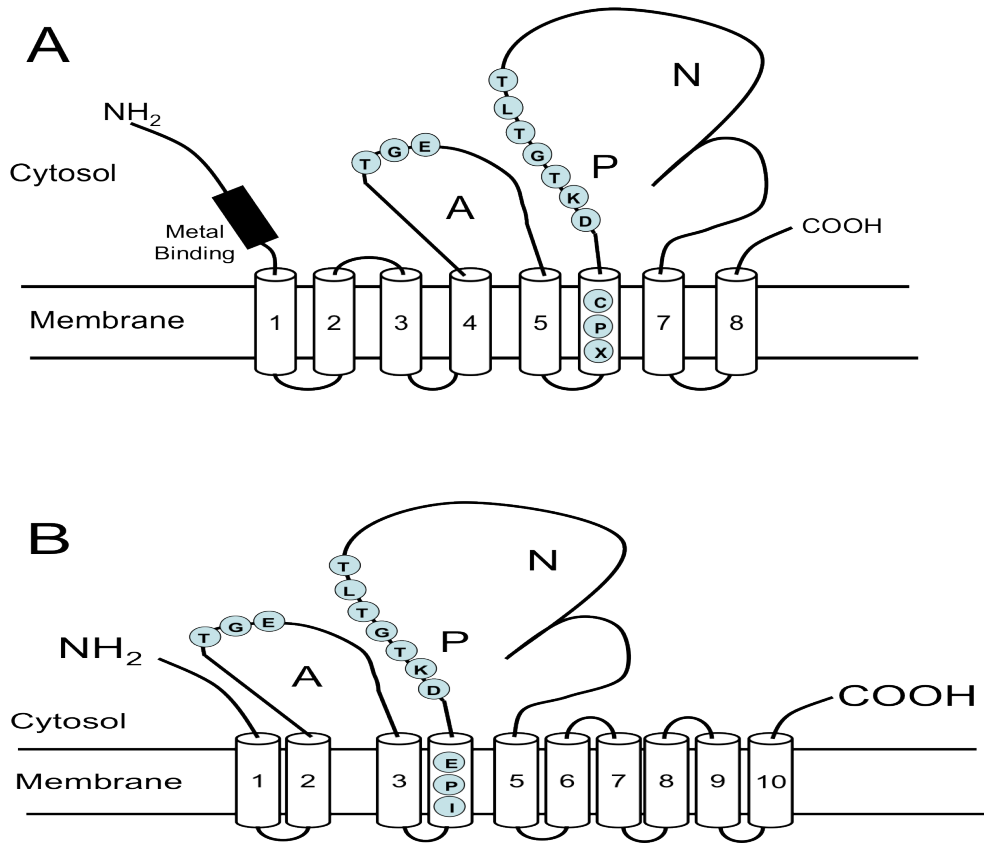
Figure 1. Scheme representing the membrane topology of a typical P$_{1B}$-ATPase (A) and a P$_2$-ATPase (B). 1–10 represent transmembrane segments. White transmembrane segments are distinct for each subgroup, black block represents N-terminal metal-binding domains, DKTGT is the consensus distinctive of the catalytic phosphorylation site. TGE is ATP-binding domain. EPI indicates amino acids identified in the SR Ca-ATPase CPX are sequences characteristic of the transmembrane metal-binding site of P$_{1B}$-ATPases.

Subgroup	Substrate category	Membrane Topology
Type 1		
1A	Bacterial KdpB ATPases	
1B	Heavy metal ATPases	
Type 2		
2A	SERCA pumps	
2B	PMCA pumps	
2C	Mammalian Na^+/K^+, H^+/K^+	
2D	Fungal pumps of uncertain function	
Type 3		
3A	HA pumps of fungi and plants	
3B	Bacterial Mg^{2+} pumps	
Type 4	Aminophospholipid transferases	
Type 5	Eukaryotic pumps of undefined function	

Table 1. Overview of the P-type ATPase Family P-type ATPase Family classification is based on that of Axelsen et al. [39] SERCA- Sarco(Endo)plasmic Reticulum Calcium ATPase, PMCA- Plasma Membrane Calcium ATPase, HA – Proton ATPase. Cations transported by the heavy metal pumps (type IB) encompass Cd^{+2}, Zn^{+2}, $Cu^{+/+2}$, Co^{+2}, Ag^+ and Mn^{+2}. Boxes indicate transmembrane segments; Filled circles, inhibitory sequences; Open circles, heavy metal binding sites.

1.4.1 P_2 and P_3-ATPases

The most characterized members of P-ATPase superfamily are P_2 and P_3 ATPases. These generate and maintain the membrane potential in eukaryotic cells via drastically changing ion concentrations on either side of the membrane. [42] These ion gradients are vital for living cells and are a driving force for secondary transport of sugars and amino acids, as well as other small molecules and ions. Although P_2 and P_3 ATPases functionally vary, as a common feature, they are consist of ten transmembrane segments. Since the membrane topology of CtpE and CtpF is similar to P_2 and P_3 ATPases, they might belong to one of these groups.

1.4.2 Substrate specificity of P_2 and P_{3-}ATPases

P_2-ATPases are the most diverse group in the P-ATPase superfamily and divided into three subgroups; P_{2A}-ATPases includes the the Sarco(endo)plasmic Reticulum Ca^{2+}-ATPase (SERCA), P_{2B}-ATPases includes plasma-membrane Ca^{2+} pumps and P_{2C}-ATPases contains the Na^+-K^+-ATPases and the gastric H^+-K^+-ATPases. During muscle contractions, SERCA in the sarco(endo)plasmic reticulum (SR) membrane pumps two Ca^{2+} ions out of muscle cells cytoplasm into the SR lumen per ATP, in exchange for two or three H^+ ions . [43] P_{2B}-ATPases Ca^{2+} pumps are also called the secretory pathway Ca^{2+} pumps (SPCA). These pumps not only transport Ca^{2+}, but also transport Mn^{2+} across Golgi membranes of plants. [44] Counter transport of ions has not been observed in these pumps. P_{2C}-ATPases contain the Na^+-K^+-ATPases and the gastric H^+-

K^+-ATPases. Na^+-pumps release three Na^+ ions in exchange for two imported K^+ ions per cycle and generate an electrical gradient across the plasma membrane in mammalian cells. [45] The Na^+ and K^+ ion gradients participate in vital cell processes such as secondary transport, signaling, and volume regulation. P_3-ATPases are H^+-pumps that are only found in the plasma membranes of plants and fungi. They are responsible for the electrochemical gradient of H^+ to regulate the extracellular pH. Similarly, H^+-ATPases sustain an intracellular pH of 6.6 against an extracellular pH of 3.5 in yeast. [46] H^+-ATPases frequently contain an autoinhibitory, carboxy-terminal extension. [42]

1.4.3   Catalytic mechanism of P_2 and P_3-ATPases

P-type ATPases undergo two distinct conformational changes called the E1 and E2 states. The E1/E2 nomenclature is also known as the Albers-Post cycle. Each of these states has a different affinity for the transported ion and nucleotide. The pumps hydrolyze ATP and transport the ion to sustain an ion gradient across the membrane. [47] The Albers-Post model describes that metals binding is required for the P-ATPases transition into phosphorylated or dephosphorylated states. According to this model, the enzyme changes its affinity for the substrate by phosphorylation, from high (E1) to low (E2). In general, the ion-translocation cycle of P-ATPases is based on the Post–Albers scheme for the Na^+-K^+-ATPase, a P_2-ATPase (Figure 3). In this model, the first ion (ion one), from the cytosol binds to a high-affinity site in the ATPase E1 state. Ion binding initiates phosphorylation of the enzyme by Mg^{2+}-ATP, which results in the phosphorylated

17

E1–P state. The phosphorylated E2–P state has a reduced affinity for ion one so it moves to the outside of the membrane. A second ion (Ion two) binds to the enzyme from outside of the membrane. Following the hydrolysis of the phosphorylated Asp residue, the enzyme releases ion two into the cell and re-binds ion one. Finally, the enzyme goes back to E1 state and is ready to start a new cycle. As a net result of this process, one type of ion is exported and another type of ion is imported per molecule of ATP consumed (Figure 2).
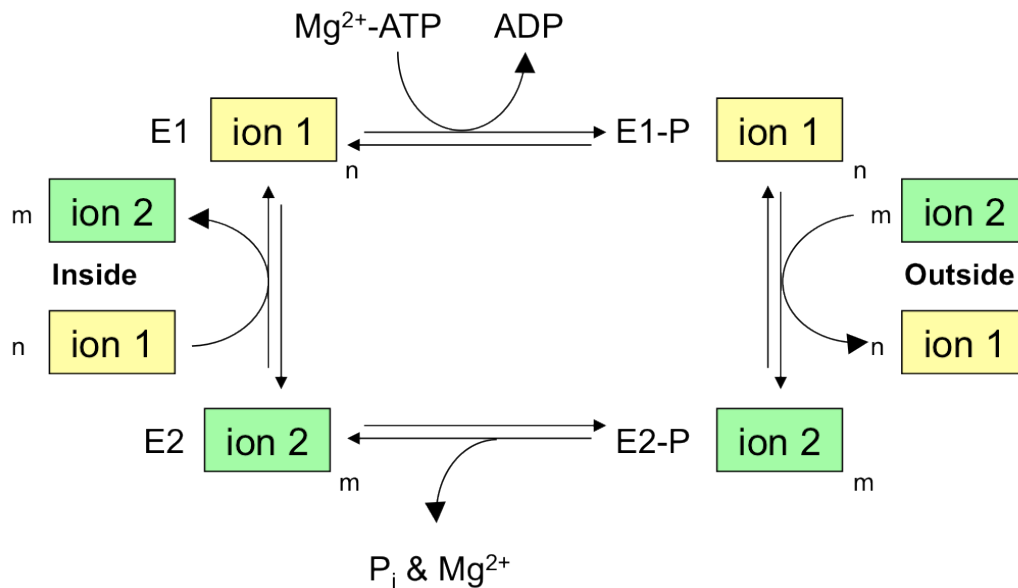
Figure 2. Catalytic Mechanism of P$_2$-ATPases. E1 and E2 represent the different conformations of the enzyme. m (ion1) and n (ion 2) represent the different cations that are transported by P$_2$-ATPases. **Inside** represents the cytoplasmic and **Outside** represents the extracellular or luminal localization of the transported metal.

All P-ATPases share a high degree of structural and functional homology, however; the molecular mechanism of transport is still unclear for many members of this large family. In other words, it is uncertain whether metal ion transport is electrogenic. The case of counter-transport has been established for a few P_2-ATPases such as the Na^+-K^+-ATPase, gastric H^+-K^+-ATPase, plasma membrane Ca^{2+}-ATPase (PMCA) and sarcoplasmic reticulum Ca^{2+}-ATPase (SERCA). [48]

1.5   P-Type ATPases in Mycobacterium species

M. tuberculosis encodes more P-ATPases than any other human pathogen. [41] Sequence analysis shows that *M. tuberculosis* encodes twelve P-ATPases; more than any other class of metal transporter in its genome. [2] These are known as Ctp   (**c**ation **t**ransporting **p**rotein). These include: one P_{1A} or KdpB-type transporter, seven probable P_{1B} or heavy metal pumps (Ctps A, B, C, D, G, J and V), four unclassifiable sequence ATPases (Ctps E, F, H and I) (Table 1). [49] All twelve *M. tuberculosis* ATPase genes are also present in *M. bovis*, another pathogen. [50] *M. marinum* genome has a similar number of P_{1B}-ATPases and atypical ATPases (Ctps E, F, H and I).[51] However, other mycobacteria such as *M. leprae*, *M. avium* and non-pathogenic *M. smegmatis* genome include five or six of these ATPases genes including only two or three P_{1B}-ATPases. This abundance of transporters might be the result of *M. tuberculosis'* evolutionary feat to adapt to its extremely harsh environmental conditions in the host phagosome. [52] This suggests that the ion transport mechanisms in *M. tuberculosis* may be critical for its virulence and microbial survival. Only a few

mycobacterial P-ATPases have been characterized such as CtpV, CtpD, CtpJ and CtpC. All of them are classified as P_{IB}-ATPases, heavy metal (Cu^{2+}, Co^{2+}, Zn^{2+}) transporters. [14, 53-55] CtpV is a Cu^{2+} transporting P_{1B}-ATPase, and required by *M. tuberculosis* to cope with copper toxicity for its survival. [53] Detailed genetic studies have showed that *ctpC* and *ctpD* genes are necessary for the optimal in vivo growth or survival of *M. tuberculosis* in a tuberculosis mouse model. [56] CtpD, a P_{1B4}-ATPase, is important for Co^{2+} and Ni^{2+} homeostasis in *M. smegmatis*. *M. tuberculosis* CtpD orthologous might be necessary for metal detoxification and its pathogenicity. [55] CtpC is a novel P-ATPase that shows Mn^{2+} activity, affects Mn^{2+} homeostasis and provides tolerance to redox stress. [14] Thereby, it exhibits a unique mechanism for Mn^{2+} metallation of secreted proteins. Reductive evolution is observed in obligate parasites because genes get inactive once their functions are not required for the pathogenic survival. As a result, the pathogen contains the minimal gene set for its virulence. [57] The *M. leprae* genome has similar transporter genes compared to *M. tuberculosis*. However, half of Ctp encoding genes in *M. leprae* are claimed to be pseudogenes. [57] If this is the case, this difference between *M. leprae and M. tuberculosis* P-ATPases genes could be due to deletion or decay of genes that are unnecessary for obligate parasitic life style of *M. leprae*. Four of the twelve P-ATPases in *M. tuberculosis* are not present at all in *M. leprae* (CtpF), and three of them are thought to be pseudogenes including CtpE, CtpH and CtpI. [57] It may be suggested that these proteins have a critical function in intra-cellular survival of *M. tuberculosis* and in

other mycobacterial species such as intra-cellular parasites. Therefore, these metal ion transporters are wroth studying during infection by *M. tuberculosis.*

ATPase Name	Subfamily	Gene name *M. tuberculosis* H37Rv	Gene name *M. smegmatis* mc^2_155	Transported ion
CtpA	P_{1B1}	**Rv_0092**	**Msmeg_5014**	Cu^+
CtpB		**Rv_0103**		
CtpV		**Rv_0969**		
CtpD	P_{1B4}	**Rv_1469**	**Msmeg_5403**	Co^{2+}
CtpJ		**Rv_3743**		
CtpC	P_{1B}	**Rv_3270**	**Msmeg_6058**	Mn^{2+}
CtpG	P_{1B}?	**Rv_1992**		**Heavy metal?**
CtpE	P_2?	**Rv_0907**	**Msmeg_5636**	**Alkali metal?**
CtpF	P_2?	**Rv_1997**	**Msmeg_3926**	
CtpH	P_2?	**Rv_0425**		
CtpI	P_2?	**Rv_0107**		

Table 2. Ctps in *M. tuberculosis* and their *M. smegmatis* orthologous. Question marks indicate that the possible P-ATPase subclass and transported ion of these enzymes. Gene names are obtained from TB Database (http://www.tbdb.org/)

1.6 Atypical Ctps in *Mycobacteria:* CtpE, CtpF, CtpH and CtpI

Axelsen *et al.* [39] analyzed 211 bacterial, archeal and eukaryotic P-ATPases and generated the phylogenetic tree according to substrate specificity despite the evolutionary distance between the parental species (Figure 5). They determined the eight conserved regions to define the core of the P-type ATPase superfamily, including TGE - phosphatase site, PEGL/CPC - ion channel motif, DKTGT - phosphorylation site, TGD-GDGXND - ATP-binding domain. According to this tree, the nine of the twelve P-ATPases in *M. tuberculosis* are classified as P_1 or P_2-ATPases; however, the rest (CtpE, CtpH and CtpI) cannot be associated with the subgroups and hence they constitute their own branches. The closest relatives of these three unclassified ATPases are the P_{3B}-ATPases of *E. coli* and *Salmonella typhimurium* (seq. 58-60), and one of the P_{2C}-ATPases from *Synechocystis* (seq. 96). The three putative P -ATPases (Ctps F, H and I) are similar to each other after the TGE sequence or 'phosphatase site' motif. It is possible that CtpF can be functionally similar to CtpH and CtpI but different in the metal stoichiometry.
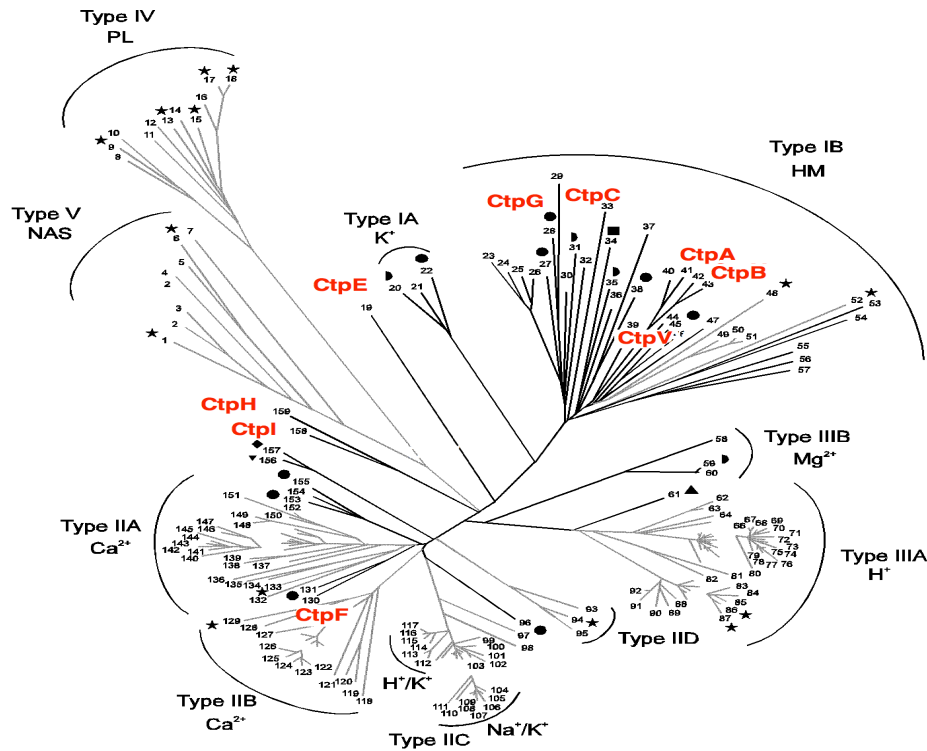
Figure 3. The Phylogenic Tree of P-ATPases (Adopted from Axelsen et al., 1998 [39]). Red marked Ctps are from *M. tuberculosis*. This tree prepared based on core sequences from 159 P-type ATPase sequences present in the EMBL and SWISS-PROT databases July 1, 1997. When the substrate specificity of the ATPases present in each family is known, it corresponds in all cases to the name of the family. The *numbers* of the sequences correspond to the numbers defined in Axelsen, K.B. & Palmgren, M.G. (1998) J. Mol. Evol. 46: 84-101,, Table 1. The numbers are always shown together with the corresponding sequences in this database. The **black branches** show ATPases originating from Bacteria and Archaea, and the **grey branches** show ATPases originating from Eukarya. The P-type ATPases from the fully sequenced organisms are shown with the following symbols: (◗) *E. coli*; (■) *Haemophilus influenzae*; (▲) *Methanococcus jannaschii*; (◆) *Mycoplasma genitalium*; (▼) *Mycoplasma pneumoniae*; (★) *Saccharomyces cerevisiae*; (●) *Synechocystis PCC6803*. The abbreviations are HM: heavy metals; NAS: no assigned specificity; PL: phospholipids.

The N-terminal regions of CtpH and CtpI are at least twice as long as its corresponding regions of other ctps. [2] This unusual aspect has not been reported previously in any other P-ATPase. Although N-terminal of CtpH and CtpI are

23

significantly different from their C-terminal halves all contain conserved residues associated with Ca^{2+} binding. The conserved motifs, XNXGE and QXXWXNXXTD are located in transmembrane segments M5 and M6 respectively. [2] Both motifs have been linked with SERCA, a Ca^{2+} binding in eukaryotic SERCA. [41] CtpH and CtpI share close homologues that both are twice as large as typical P-ATPases and contain an internal fusion with the C-terminal half preserving all functional motifs, but which are lacking in the N-terminal half [50]. This suggests that rapid gene gain and loss occurred during *M. tuberculosis* evolution. Another study analyzed 68 P-type ATPase in Actinobacteria phyla, *M. tuberculosis* and identified conserved sequences in Actinobacteria important for ATPase activity. [50] Although sequences of CtpE, CtpH and CtpI do not reveal their substrate specificity, they function as ATPase in the cell.

Eukaryotic counterparts of these functionally uncharacterized proteins, CtpE, CtpF, and C-terminal halves of CtpH and CtpI have P_2-ATPases membrane topology. CtpF clusters with eukaryotic Golgi Ca^{+2} -Mn^{+2} ATPases (SPCA1) and its close relative PMR1, Golgi ATPase, in yeast [50] [41]. Bioinformatics studies indicate CtpE has around 20% homology to Ca^{+2} -Mn^{+2} -ATPases and P_{3A} ATPases, while CtpF is 33% homologous to Ca^{+2} -Mn^{+2} ATPases. CtpH is 27% homologous to P_{3A} ATPases and CtpI is 20% homologous to Ca^{+2} -Mn^{+2} -ATPases and 19% homologous to P_{3B}-ATPases. [50]

In conclusion, experimental verification is required to determine substrate specificity and cellular roles of these novel ATPases, CtpE, CtpF, CtpH and CtpI.

2   MATERIALS AND METHODS

2.1   Strains and culture conditions

M. tuberculosis H37Rv and *M. smegmatis* mc²155 were used in this study. All mycobacterial strains were grown in Sauton' s or 7H9 liquid media, and 7H10 agar plates (BD-Difco), supplemented with 0.5% bovine serum albumin, 0.2% Dextrose and 0.05% Tween 80 (ADT). *E.coli* BL21 (DE3) pLysS or Top10 cells transformed with the plasmid pSJS1240 coding for rare tRNA (tRNA argAGA/AGG and tRNA ileAUA) [14] were grown at 37 °C in 2XYT or at 20 °C auto-induction medium containing 50 µg/ml spectinomycin, 34 µg/ml chloramphenicol and 100 µg/ml ampicillin.

2.2   Mutant Strains Preparation

The *M. tuberculosis ctpE::Hyg and ctpF::Hyg* mutant strains were constructed by replacement of the coding sequence of *ctpE and ctpF* genes (locus tag Rv0908 and Rv1997, respectively) with a hygromycin resistance (hygR) cassette. Genes were amplified from *M. tuberculosis* genomic DNA containing of a 1000 bp fragment corresponding to the 5'- first 500 bp and 3'- last 500 bp flanking regions. 5'UTR and 3'UTR regions amplified with restriction sites with SpeI / NotI and ApaI / XhoI. Consequently, they were inserted into upstream and downstream regions of the cassette. The product containing the hygR cassette bordered by ~ 500 bp of the 5' and 3' flanking regions of both genes were transformed into electrocompetent *M. tuberculosis* H37Rv harboring plasmid pJV53 and induced with 0.02% acetimide for 8 hrs. [58] The cultures were treated

with 0.2 M glycine for 8 hours before making electrocompetent cells before transformation. Transformants were selected on 50 µg/ml hygromycin and 25 µg/ml kanamycin supplemented 7H10-ADC plates. The presence of *ctpE and ctpF* insertional mutations was analyzed by PCR amplification of the hygR cassette flanked by the N- and C- terminal junctions. *M. tuberculosis* cell culture steps were carried on at BSL-3 level, UMASS Medical School. All primer used are listed in Appendix. Mutant strains of *M. smegmatis* for *ctpE::Hyg and ctpF::Hyg*, used in this study were generated similarly previously by Dr. Daniel Raimunda*.*

2.3 Complemented Strains Preparation

For the complementation of M*. smegmatis ctpE::Hyg and ctpF::Hyg,* the *M. smegmatis ctpE and ctpF* were amplified from genomic DNA with restriction sites, HpaI and KpaI. The resulting PCR fragments were digested and ligated into pJEB402 plasmid resulting in pJEB402-MsmE and pJEB402-MsmF. The ligation reactions were transformed into DH5α cells and plated on 2XYT agar plates supplemented with 25 µg/ml kanamycin. After overnight incubation at 37 °C, the presence of the insert was verified by colony PCR with gene specific primers. The plasmids were then isolated from 5 ml culture of candidate colonies by NucleoSpin® Plasmid QuickPure (MACHEREY-NAGEL) according to manufacturer's instruction. The presence of inserts was verified this time with double restriction enzyme digestion. For double digestion of constructs, two single cutter restriction enzyme sites, HpaI and KpnI, were picked via NEB cutter

V2.0 software (http://tools.neb.com/NEBcutter2/). HpaI restriction site is located in the gene and KpnI restriction site is located in the vector. Confirmed vector constructs were electroporated into the corresponding mutant strain and transformants were selected on 25 µg/ml kanamycin, 7H10-ADC and verified by PCR using primers matching inside the gene.

2.4 Metal, redox stressors and pH sensitivity assays

Metal sensitivity was assayed, *M. smegmatis* mc^{2}155 wild type, *M. smegmatis ctpE::Hyg and ctpF::Hyg* and complemented strains in Sauton's media containing different concentrations of $NiCl_2$, $CaCl_2$, $MgCl_2$, $NaCl$, $CuCl_2$, $CoCl_2$, $MnCl_2$, $ZnSO_4$, $FeCl_3$ or $CdCl_2$. As redox stressors Dithiothreitol (DTT), Paraquate, Potassium cyanide (KCN), Benzamidine were used. For pH sensitivity assays, Sauton's media was buffered 25 mM MES (Sigma) or TRIS (Sigma). pH was adjusted with NaOH or HCl. All cultures were inoculated at OD_{600} of 0.1 from late exponential phase cultures and supplemented with the desired metal concentration as specified in the figures. Cells we incubated for 24 hrs. and OD_{600} measured.

2.5 Gene expression analysis

Mycobacterium smegmatis mc^{2}155 cells in exponential phase were supplemented with 500 µM $CoCl_2$, 500 µM $NiCl_2$, 500 µM $CuCl_2$, 1 mM $ZnCl_2$, 1 mM $MgCl_2$ 1 mM $CaCl_2$ or 1 mM $MnCl_2$. All redox stressors were added 100 µM. Then, cultures incubated for 2 hrs. Cells were harvested, resuspended in

1 ml of TRIzol reagent (Invitrogen, Carlsbad, CA) and disrupted using Lysing Matrix B (MP Biomedicals) in a cell disrupter (FastPrep FP120, Qbiogene, Carlsbad, CA). RNA pellets were air dried and redissolved in 30 µl of diethyl pyrocarbonate-treated ultrapure water. Remaining DNA was removed with RNeasy minikit and an on-column DNase I kit (Qiagen, Valencia, CA). The RNA samples (1 µg) were used as template for cDNA synthesis with random primers and SuperScript III reverse transcriptase (Invitrogen, Carlsbad, CA). For transcript analysis of *ctpE* and *ctpF* semi quantative RT-PCR was performed with primers qCtpE-F/R and qCtpF/R. Primers qSMEG-2758sigA-F and qSMEG-2758sigA-R were used to amplify the RNA polymerase sigma factor (*sigA*), as an internal reference. The products of sq RT-PCR were visualized on 1.2% agarose gel containing 1 µg/ml ethidium bromide. Density analysis of agarose gels were analyzed and quantified via Quantity One 1-D Analysis Software (Bio Rad). Determinations were completed with RNA extracted from three independent biological samples.

2.6   CtpE and CtpF cloning and heterologous expression

The *ctpE and ctpF* genes were amplified from *M. tuberculosis* H37Rv and *M. smegmatis* mc^{2}155 genomic DNA using the primers Mtb *ctpE* Fwd and Rvs, Mtb *ctpF Fwd and* Rvs and Msm *ctpE* Fwd and Rvs, Msm *ctpF Fwd and* Rvs. These introduced a Tobacco Etch Virus (TEV) protease site-coding sequence at the amplicon 3' end. The resulting amplicon was cloned into pBAD or pEXP5-NT TOPO/His vector (Invitrogen) which introduces a carboxyl- or amino terminal

(His)$_6$ tag suitable for Ni^{2+} affinity purification. Used primers are listed in Appendix A. Sequences were confirmed by automated DNA sequence analysis and restriction enzyme digestion. *E.coli* BL21 (DE3) pLysS pSJS1240 or Top10 cells were transformed with these plasmids. Cells were grown at 37 °C in 2XYT medium or 30 °C in ZYP-505 media supplemented with 100 µg/ml ampicillin, 50 µg/ml spectinomycin, and 34 µg/ml chloramphenicol. Protein expression was induced with 0.002% L-arabinose for pBAD or 0.5 mM Isopropyl β-D-1-thiogalactopyranoside (IPTG) for pEXP5-NT. Cells were harvested 3 hrs. after induction, washed with 25 mM Tris, pH 7.0, and 100 mM KCl and stored at −80 °C. Alternatively, cells were grown at 30 °C in ZYP-505 media supplemented with 0.05% α-lactose monohydrate, 100 µg/ml ampicillin, 50 µg/ml kanamycin. [59] Cells were harvested at 24 hrs. post inoculation, washed with 25 mM Tris, pH 7.0, 100 mM KCl and stored at −80 °C.

2.7   Heterologous purification of CtpE and CtpF from

Protein purification was performed as previously described [60] with minor modifications. All purification steps were carried out at 0–4 °C. Cells were suspended in buffer A (25 mM Tris, pH 7.0; 100 mM sucrose; 1 mM phenylmethylsulfonyl fluoride (PMSF, Sigma) and disrupted with a French press at 20,000 psi. Lysed cells were centrifuged at 8,000x *g* for 30 min. The supernatant was then centrifuged at 229,000x *g* for 1 hr. and the pelleted membranes were resuspended in buffer A (10–15 mg/ml). For protein solubilization and purification, membranes were diluted to a final concentration of

3 mg/ml in buffer B (25 mM Tris, pH 8.0; 100 mM sucrose; 500 mM NaCl; 1 mM PMSF) and solubilized with 0.75% dodecyl-β-D-maltoside (DDM, Calbiochem). The preparation was incubated for 1 hr. at 4 °C with mild agitation. The solubilized membrane protein suspension was cleared by centrifugation at 163 000 g for 1 hr. The supernatant was incubated for 1 hr. at 4 °C with Ni^{2+}-nitrilotriacetic acid resin (Ni-NTA) (Qiagen) pre-equilibrated with buffer B, 0.05% DDM, and 5 mM imidazole. The resin was washed with buffer B, 0.05% DDM containing 10 and 20 mM imidazole and the protein was eluted with buffer B, 0.05% DDM, 250 mM imidazole. Fractions were pooled, concentrated, and buffer replaced by 25 mM Tris, pH 8.0; 100 mM sucrose; 50 mM NaCl and 0.01% DDM (buffer C) using 30 kDa cut-off centricons (Millipore). The proteins were aliquoted and stored in 20% v/v glycerol at −20 °C until use. All protein concentrations were determined by Bradford method. [61] Purified protein was analyzed by 10% SDS-PAGE followed by Coomasie brilliant blue (CBB) staining or western blot using an anti-(His)$_6$-tag antibody (GenScript).

2.8   p-Nitrophenyl Phosphatase (pNPPase) Activity Assays

pNPPase activity assays were carried out as previously described with modifications. [62] pNPPase activity was performed in a mixture containing: 60 mM p-nitrophenyl phosphate (pNPP), 50 mM MES (pH 5 or 6 at 37 °C) or 50 mM Tris (pH 7.4, 8 or 9 at 37 °C), 3 mM $MgCl_2$, 0.01% asolectin, 0.01% DDM, 50 or 400 mM NaCl, 0.01 or 0.05 mg/ml purified enzyme, and 0, 2, 10, 20 or 50 mM Cystein concentrations. The buffer was prepared at room temperature and pH 7.

pNPPase activity was measured for 10 min at 37 °C. As control, 0.01 or 0.05 mg/ml CopA was used as described previously. pNPP hydrolysis was estimated by measuring the absorption of p-nitrophenol at 410 nm after adding 4 volumes of 0.5 N NaOH (ε = 17000 M^{-1} cm^{-1}).

2.9 Bioinformatics Analyses

M. tuberculosis CtpE and CtpF protein sequence was used for a BLAST search against all predicted sequence in the NCBI database. Resulting homologous sequences were aligned with MUSCLE [63] and ESPript [64] software. The membrane topology of proteins was determined by TMHMM Server v. 2.0 (**http://www.cbs.dtu.dk/services/TMHMM/**).[65] For protein modeling, UniProtKB/Swiss-Prot and the PyMOL Molecular Graphics System, Version 1.5. 0.4 Schrödinger, LLC were used. [66]

3 RESULTS

3.1 Bioinformatics analysis of CtpE and CtpE from *M. tuberculosis*

In our study, we focused on understanding cellular functions of atypical ATPases*:* CtpE and CtpF in *M. tuberculosis*. In order to reveal possible functions, CtpE and CtpF sequences were analyzed in relation to their conserved residues found on the transmembrane helices. Both CtpE and CtpF have ten transmembrane segments. Therefore, they are similar to P_2 and P_3-ATPases based on their membrane topology (Figure 4 A, B). Both of them contain essential motifs that are involved in phosphatase (TGE), phosphorylation (DKTGT), and ATP-binding (TGD-GDGXND) activity. These motifs are essential for a functional P-ATPase.

In P_2-ATPases, alkali metal transporters, TMs M4, M5, and M6 participate in metal binding and transport, with key residues conserved among those enzymes with identical ion selectivity. [39] Thereby, we analyzed those TMs of CtpE and CtpF. Transmembrane segments of CtpF contain conserved residues associated with Ca^{2+} binding. The conserved motifs, VAXIXPE, NXXE and NXXTD are located in transmembrane segments M4, M5 and M6 respectively. [41] P_{2A}-ATPases have two and P_{2B}-ATPases have one Ca^{2+} binding sites. Residues at M4 and (N) at M6 are associated to multiple Ca^{2+} binding sites. [41] CtpF contains these residues; thereby, it is possible that it transports alkali metal like Ca^{2+} (Figure 5).

CtpE also exhibits similar membrane topology to P_{2A}-ATPase, and contains PEGL in the M4 that is common for all P_2-ATPases. On the other hand, it holds

neither heavy metal signature motifs (CPX) nor the SERCA associated M5/M6 motifs (Figure 4 B). Therefore, CtpE cannot be associated any class of P-ATPases.
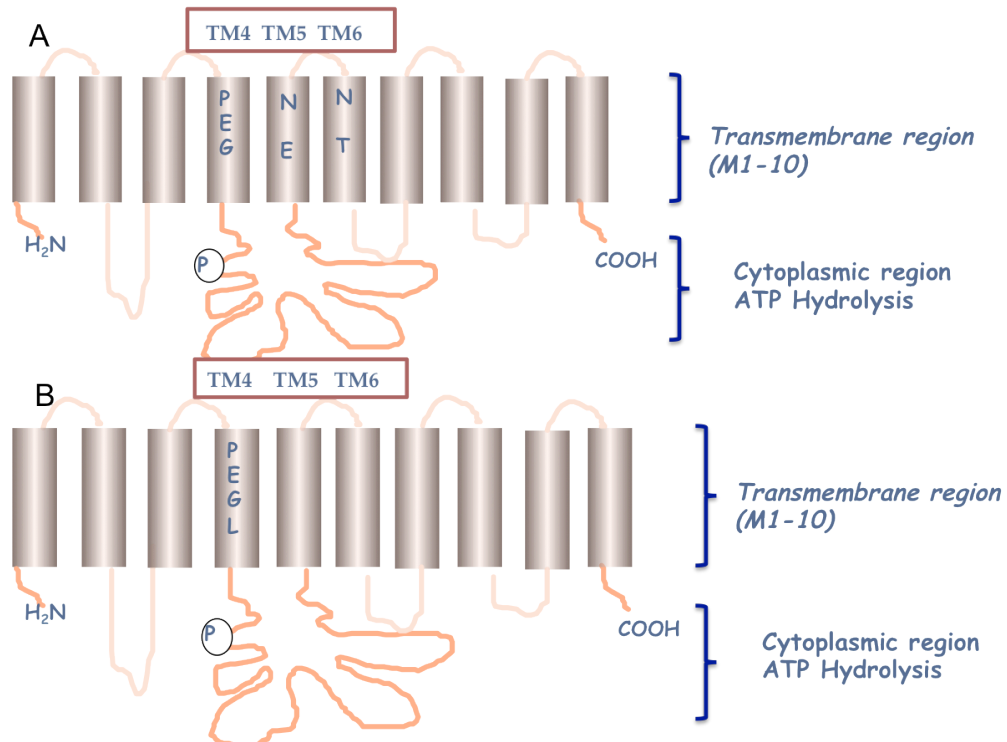
Figure 4. A schematic representation of the membrane topology of CtpF (A) and CtpE (B) from *M. tuberculosis.* Trans membrane helices, M1-10, are determined by TMHMM Server. The relative locations and structure of phosphorylation (P) is shown. The conserved amino acids in TM4, TM5 and TM6 forming the transmembrane metal binding domain is indicated by red frame. (A) Residues, on the TM4, TM5 and TM6 of CtpF, are associated with Ca^{+2} transport and form a putative Ca^{+2} binding pocket. (B) The PEGL motif is common in P_2-ATPases that is located on the TM4 of CtpE.

Since transmembrane segments are associated with the ion specificity of P-ATPases, CtpE and CtpF sequences were aligned with previously classified two Ca^{+2} transporters with respect to their ion binding sites. Primary sequences of

CtpE and CtpF from *M. tuberculosis,* compared to two different Ca^{2+} ATPases, *Oryctolagus cuniculus* Serca1, and *Listeria monocytogenes* (LMCA1). (Figure 5A) Two Ca^{2+} binding sites of eukaryotic Ca^{2+} ATPases (Serca 1, PDB ID: 1T5T) were shown by its crystal structure. [67, 68] In contrast, LMCA1 from *L. monocytogenes* contains only one Ca^{2+} binding sites. [69] Transmembrane segments (TM4, TM5, TM6) of CtpE and CtpF were analyzed with respect to their putative Ca^{2+} binding residues (Figure 5 A). CtpE does not hold any of the conserved residues except the glutamate in the PEGL motif at TM4. On the contrary, CtpF contains five important Ca^{2+} binding residues. Similarity in these residues may suggest that CtpF has an alkali metal binding site between TM4, TM5, and TM6. To visualize the location of these conserved residues, the structural models of CtpE and CtpF were generated. Most of the residues are necessary to transport Ca^{2+} were observed at in between CtpF TM4, TM5, and TM6. For instance, residues like V^{286}, I^{289}, E^{291} at TM4, N^{709} at TM5 and N^{736} at TM6 seem like creating a metal binding platform for a possible ion transport (Figure 5 C). A similar phenomenon was not observed at CtpE (Figure 5 B).

Figure 5. Bioinformatics analysis of CtpE and CtpF from *M. tuberculosis.* (A) Partial alignment of CtpE and CtpF homologous proteins sequences corresponding to TM4, TM5 and TM6. Black arrows indicate conserved residues for Ca^{+2} binding. Sequences are from Rv0908 and Rv1997 M. tuberculosis; ATP2A1 *Oryctolagus cuniculus* and lmo0841 *Listeria monocytogenes.* (B,C) Homology models of CtpE and CtpF generated with UniProtKB/Swiss-Prot. Blue and green TMs are the putative metal binding pockets.

3.2   CtpF, CtpE and CtpG gene disruptions in Mycobacterial genomes causes phenotype:

To identify the functional role of two putative P-ATPases, CtpE and CtpF, from *M. tuberculosis* insertional mutants (*ctpE::Hyg, ctpF::Hyg)* were generated. In addition, a *ctpG::Hyg* mutant was made in parallel. CtpF, CtpE and CtpG encoding genes in both species were successfully interrupted with an antibiotic resistance (*Hyg^R*) gene insertion as described Methods section 2.2. To this end, a *Hyg^R* cassette-containing vector was constructed with 5' and 3' UTR flanking

regions of *ctpF, ctpE* or *ctpG* by sequential cloning of these regions. Afterward, vectors were electroporated into *M. tuberculosis* wild type cells and allowed to homologous recombination. The proper construction of plasmids and insertion mutants (*ctpE::Hyg , ctpF::Hyg* and *ctpG::Hyg)* were verified by PCR and restriction enzyme digestion (Figure 6). Insertion mutations of *M. tuberculosis* are ready for a further analysis under various stressor conditions and compared with wild type. These will be completed in the future by other members of Argüello's lab.
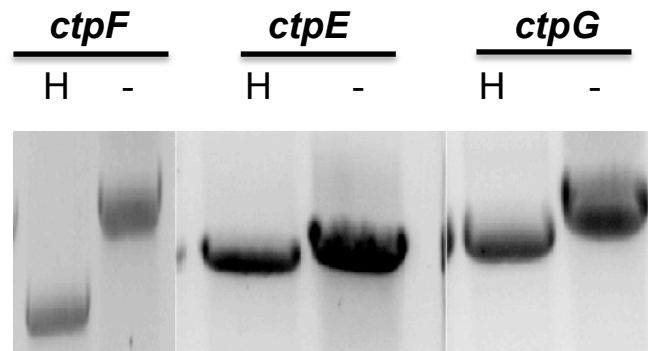

Figure 6. PCR verification of Hygromycin cassette inserted *ctpF, ctpE, ctpG* genes on 1% Agarose gel. **H** indicates *Hyg^{R}* inserted genes. **–** shows full-size genes amplified from wild type cells. The size difference between mutant and WT indicates a successful insertion of the *Hyg^{R}* into these genes.

3.3 *M. smegmatis* ctpE::Hyg insertion mutant has sensitivity to alkali pH

M. smegmatis is commonly used as a model organism for tuberculosis studies. Moreover, it contains *M. tuberculosis* CtpE and CtpF orthologous. Thereby, we tested the response of *M. smegmatis ctpE::Hyg* and *ctpF::Hyg* insertion mutants

to various pH levels. Results showed that *M. smegmatis* lacking of *ctpE* was sensitive to alkali pH (Figure 7). On the other hand, *M. smegmatis* lacking of *ctpF* behaved similar to wild type cells. (Data not shown) Our result suggests that CtpE putative P-ATPase that could play a role in pH homeostasis of *M. smegmatis* and *M. tuberculosis*.
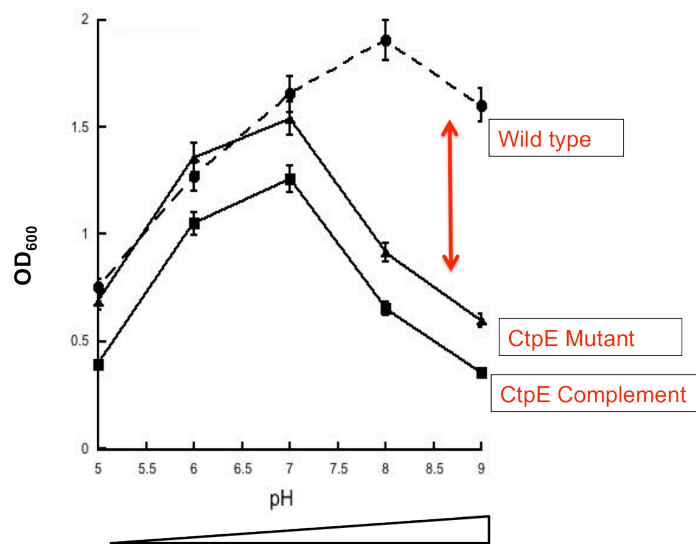

Figure 7. pH sensitivity assay of *M. smegmatis* ctpE::Hyg insertion mutant. *M. smegmatis* lacking of ctpE cells showed sensitivity to alkali pH. Cells were cultured 24 h in liquid Sauton' s media in different pH as indicated. Cell growth is quantified by measuring OD_{600}. Data are the mean ± SE of three independent experiments.

3.4   CtpE and CtpF mutant of *M. smegmatis* are sensitive to Mn^{+2}

To study the functional role of CtpE and CtpF in *M. smegmatis*, we evaluated the in vitro survival of *M. smegmatis ctpE::Hyg* and *ctpF::*Hyg insertion mutants and their complemented strains in the presence of various metal stressors. As a

result, *ctpE::Hyg* and *ctpF::*Hyg were more sensitive to millimolar concentrations of Mn^{+2} than the wild- type cells (Figure 8). On the contrary, the complement *M. smegmatis ctpE::Hyg* and *ctpF::*Hyg strains behaved similar to wild type, thus these strains could not recover the function of CtpE in *M. smegmatis* mutant cells. Nevertheless, Mn^{+2} sensivity of *M. smegmatis* lacking of *ctpE and ctpF* suggests that CtpF and CtpE may contribute the detoxification of high levels of Mn^{+2} from the cell for its survival.

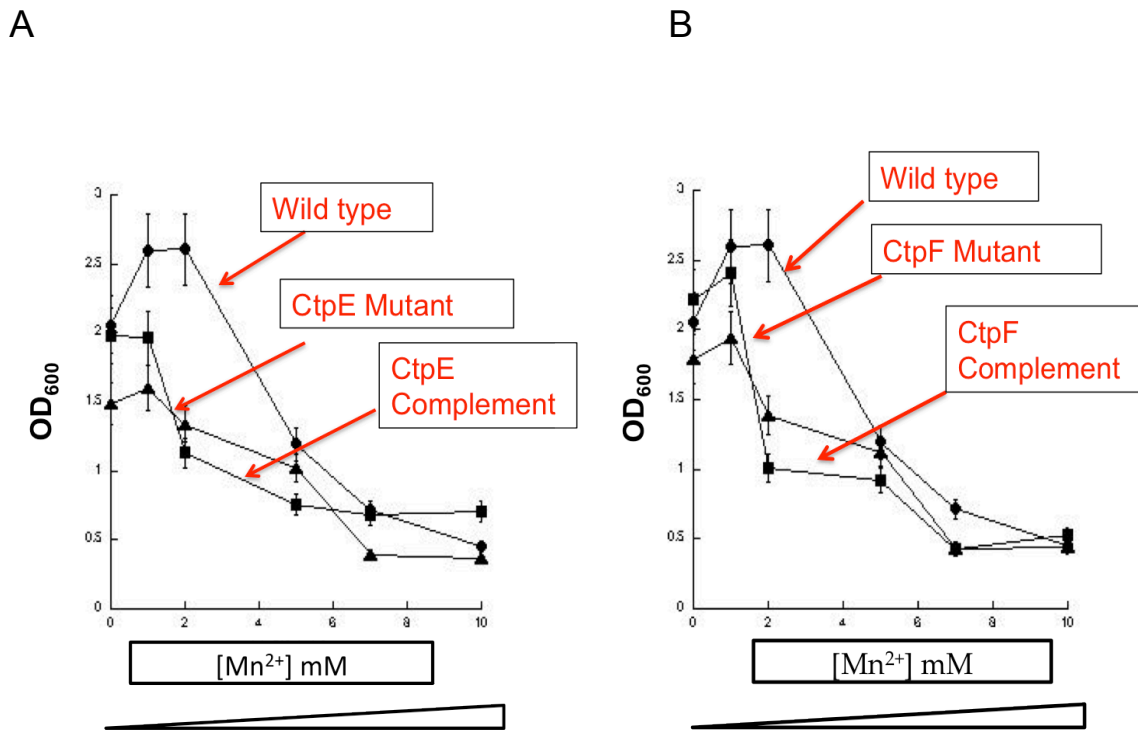**Figure 8. Mn^{+2} sensitivity assay of *M. smegmatis* ctpE::Hyg (A) and ctpF::Hyg (B) insertion mutants. Both mutants showed higher sensitivity to Mn^{+2} than the wild-type cells**. Cells were cultured 24 h in liquid Sauton' s media in increased concentration **Mn^{+2}** as indicated. Cell growth is quantified by measuring OD$_{600}$. Data are the mean ± SE of three independent experiments.

Since natural substrates and functional roles in the cell of CtpE and CtpF putative P-type ATPases are unknown, mutant strains were exposed to various metal stressors (NiCl$_2$, CaCl$_2$, MgCl$_2$, NaCl, CuCl$_2$, CoCl$_2$, MnCl$_2$, ZnSO$_4$, FeCl$_3$ and CdCl$_2$) and oxidative stressors (DTT, Paraquate, KCN, Benzamidine). A difference was not observed between WT and M. *smegmatis ctpE::Hyg* and *ctpF::*Hyg insertion mutants growth under these stressors (data not shown), suggesting that these would not be in vivo substrates of these transporters.

3.5 Construction of complemented strains of *M. smegmatis ctpE::Hyg* and *ctpF::*Hyg insertion mutants

To investigate the physiologic roles of CtpE and CtpF from *M. smegmatis* and *M. tuberculosis* at cellular level, protein-encoding genes were disrupted with Hyg^R cassette. *M. smegmatis* mutant strains could not survive under some stress conditions (see section 3.2 and 3.3). To recover phenotypes of mutant strains, a vector (pJEB402) containing the strong constitutive mycobacterial optimal promoter [70] were successfully constructed. The proper construction of pJEB402 plasmids verified with digestion enzymes, HpaI and KpnI (Figure 9). Then, these constructs inserted into M. *smegmatis ctpE::Hyg* and *ctpF::*Hyg strains via electroporation as described in detail at Section 2.3. The insertion of constructs verified by PCR using the gene specific primers (Figure 10). These complemented strains were further analyzed under same stress conditions applied for mutant strains regarding. Complemented strains were not able to recover phenotypes observed for M. *smegmatis ctpE::Hyg* and *ctpF::*Hyg.
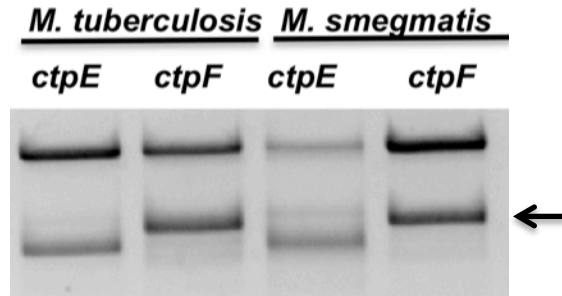
Figure 9. Restriction enzyme digestion verification of ctpF, ctpE genes inserted pJEB402 constructs. All constructed plasmids double digested with HpaI and KpnI. **Narrow** indicates double digestion products.
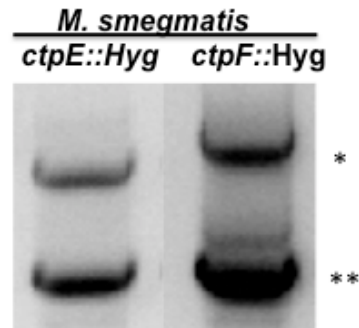
Figure 10. Colony PCR from pJEB402 inserted *M. smegmatis ctpE::Hyg* and *ctpF::*Hyg strains (complemented strains). Lower bands (**) are hygromycin casette with ~500 bp flanking regions of *ctpE* and *ctpF*, respectively in genome. Higher bands (*) are full l-length *ctpE and ctpF* genes in pJEB.

3.6 Transcriptional level changes in *ctpE* and *ctpF* genes in *M. smegmatis* under different stress conditions

Semi quantitative reverse transcription polymerase chain reaction (sq RT-PCR) was performed to screen *ctpE* and *ctpF* gene expression changes in *M. smegmatis* under stress conditions. *M. smegmatis* (Mc^2 155) wild- type exposed to various metals, pH and redox stressors as specified section 2.2. To determine

gene expression levels, total RNAs isolated from those and used as a template for cDNA production. The gene segments were amplified from these cDNAs and the quantity of PCR products were analyzed on agarose gels regarding to their intensity. *ctpE* and *ctpF* expression levels were normalized with a house keeping gene (*sigA*). A statistically significant induction of *ctpE* or *ctpF* mRNA was not observed upon exposure to metals (Mn, Ca, Zn, Ni, Co, Cu, Mg), oxidative stressors (DTT, Paraquate, KCN,), ammonium acetate or various pHs (Figure 11) based on density analysis of PCR product containing agarose gel.
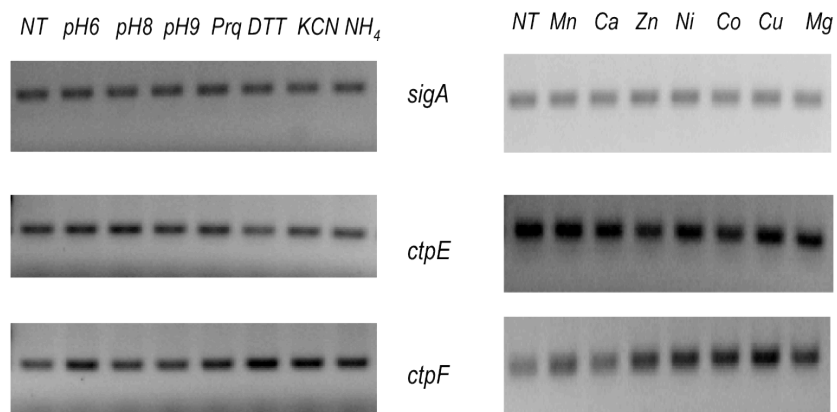
Figure 11. A sample gel for the transcriptional response of *ctpF* and *ctpE*. Various pH, redox and metal stressors were tested by semi-quantitative RT-PCR. The RNA polymerase sigma factor (*sigA*) used as an internal reference. The same amount of samples was run on same size 1.2% agarose gels. Determinations were carried out with RNA extracted from three independent biological samples. Abbreviations as are; NT: Non-treated, Prq: Paraquate, DTT: Dithiothreitol, KCN: Potassium cyanide NH$_4$: Ammonium acetate.

3.7 Cloning and heterologous expression of *M. smegmatis ctpE* and *ctpF*

ctpE and *ctpF* from *M. smegmatis* were cloned into pBAD and pEXP5-NT-TOPO vectors, generating *CtpE_Msm_pBAD* and CtpF_Msm_*pEXP5-NT* respectively. The presence of genes in vector constructs was verified by PCR with gene specific primers and then restriction enzyme digestion using PpuMI and BstZ17 (Figure 12).
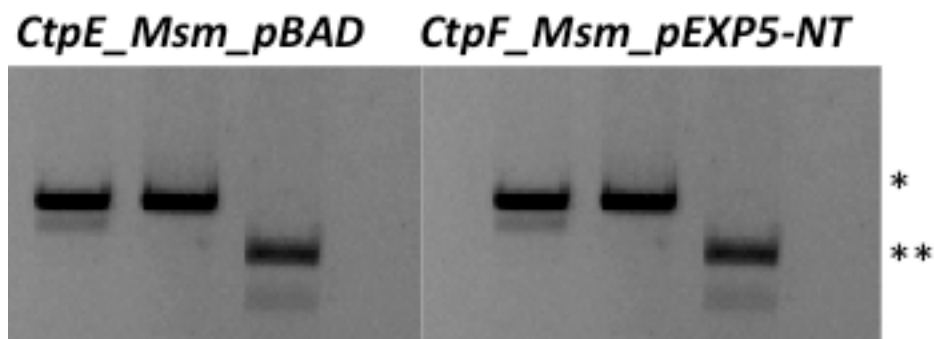
Figure 12. Expression vector constructs of CtpE and CtpF. CtpE_Msm_pBAD and CtpF_Msm_pEXP5-NT constructions verified with double restriction enzyme digestion with respect to their insertion genes. * indicates that the single digest with either PpuMI or BstZ171, **: Double digest with PpuMI and BstZ171 to verify the correct gene insertion. 1% Agarose gel was used to visualize digestion products.

Recombinant CtpE and CtpF proteins were expressed in various *E.coli* strains. In order to obtain the best yield of proteins, various expression cell lines (BL21 DE3, BL21 DE3*Star,* BL21 DE3 pLysS pSJS1240, Top10 or Rosetta) were tested using 2XYT or autoinduction media. Cultures were incubated at various temperatures (20, 30 or 37 °C) and durations (4, 8 or 16 hrs.) supplemented with different concentrations of L-arabinose (0.2, 0.02, 0.002%) or IPTG (0.5-1 mM).

The best expression of recombinant CtpE and CtpF was observed with BL21 DE3 pLysS pSJS1240 cell line using 2XYT media induced with % 0.002 Arabinose for 4 hrs. at 37 °C and auto induction media with % 0.05 α-lactose at 20 °C for 16 hrs.

3.8 Heterogously purified *CtpE* from *M. smegmatis* did not show phosphatase activity under tested conditions

Following the heterologous expressions of CtpE in *E.coli*, recombinant proteins were purified by Ni^{2+}-NTA affinity column. This purification method generated pure CtpE as analyzed by Coomassie Brilliant Blue-stained SDS-PAGE gel (Figure 13). The immunostained western blot of the same process verified that CtpE protein was obtained (Figure 13). The approximate yield for CtpE was 1 mg/L of cell culture. The purified protein was used for further analysis of enzyme activity assays.

P-nitrophenyl phosphatase (pNPPase) activity assay was used to confirm that the purified enzyme is active P-nitrophenyl phosphate (pNPP) and it is a commonly used substrate for alkaline phosphatases. This assay provides colorimetric estimation of the p-nitrophenol released by phosphatase activity. The pNPPase activity for CtpE was assayed under various conditions such as various pH, salt or cysteine concentrations. Heterogeneously purified CtpE did not show phosphatase activity under any of these conditions.
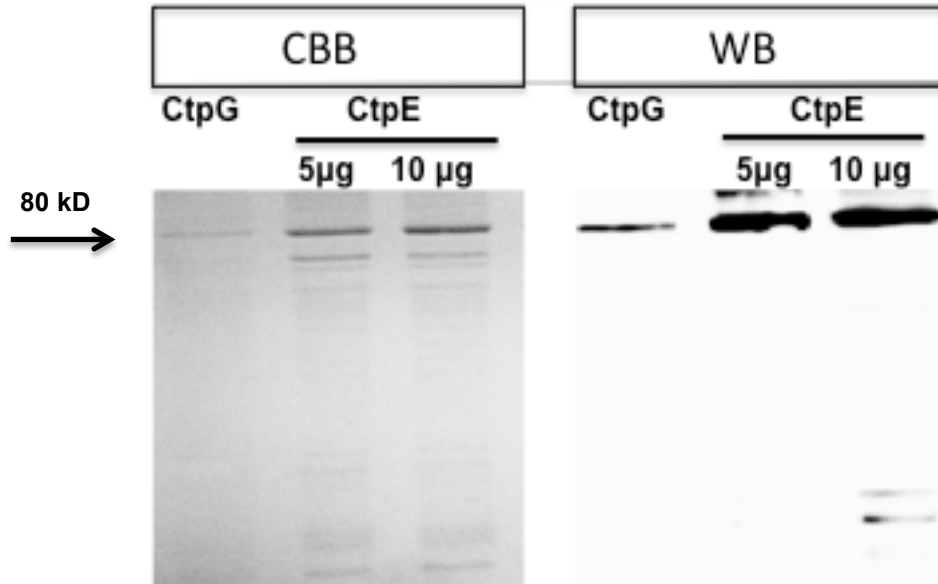
Figure 13. Heterogeneously expressd and purefied CtpE . Histidine tagged CtpG (1 µg) from
M. tuberculosis was used a positive control. 5 µg and 10 µg of total CtpE protein were loaded on
10 % SDS-PAGE and the gel was visualized by Coomassie Brilliant Blue-staining (CBB). (WB) is
the western blot of the corresponding gel with Histidine antibody. Heterogeneously purified CtpE
was pure enough to further experiments.

Similar to CtpE, CtpF from *M. smegmatis* was expressed in *E.coli* and purified by
Ni^{2+}-NTA affinity column. All purifications steps were analyzed Coomassie
Brilliant Blue-stained SDS-PAGE gel and immunostained western blot with
previously prepared CtpG as positive control. Several non-specific bands were
observed on purified CtpF SDS-PAGE gel. Following immunostaining for
hexahistidine group analysis indicated that purified process of CtpF resulted with
highly degraded protein. Optimization trials of CtpF purification processed
resulted similarly. Therefore, purified CtpF could not be used for further assays
such as enzyme activity.

.

4   CONCLUSION

The genome analysis of *M. tuberculosis* indicates that it has twelve P- ATPases. This unusual number of transporters in the genome may indicate that *M. tuberculosis* evolved to cope with harsh conditions in the host it encounters. Moreover, orthologous of CtpE and CtpF are also found in *M. smegmatis*, which is a non-pathogenic mycobacteria species, and share 36% homology. Containing two copies of a P- ATPase is not a common phenomenon among bacteria. This could be due the physiological importance of these genes for mycobacterial survival. Two of them, CtpE and CtpF are putative novel ATPases with unknown natural substrates. In this study, we analyzed their physiological roles in the cell. Our bioinformatics study showed that their membrane topologies are similar to P_2- ATPases, composing of ten transmembrane segments. In addition, both have PEGL motif at TM4 that are common for alkali metal transporters. These observations suggest that CtpE and CtpF could be classified as P_2- ATPases.

To reveal the functional role of these proteins in the cell, we successfully generated strains of *M. tuberculosis* and *M. smegmatis* that are lack of CtpE or CtpF. We also constructed complemented strains of these mutants by a mycobacterial optimal promoter containing plasmid. These strains were tested under different pH, redox stressor and metals. Our sensitivity test showed that *M. smegmatis* was not able to cope with alkali pH levels in absence of *ctpE* gene. Managing acidic pH is essential for the survival of some mycobacterial species including *M. tuberculosis* and *M. smegmatis*. Yet, there is not a very well defined pH-regulation mechanism reported in mycobacterial species. It may be

suggested that CtpE has a role in the internal pH regulation of *M. smegmatis.* Some conserved residues in P-ATPases are generally consistent with the metal they transport such as CPX is found in P_{IB}-type. CtpE and CtpF do not contain any known consensus sequences to predict their substrate. Therefore, a large selection of metal ions was tested on the growth of M. *smegmatis ctpE::Hyg* and *ctpF::*Hyg insertion mutants. The results showed that none of them except Mn^{2+} had an effect on them. Mutant strains when compared to wild type cells died lower concentration of Mn^{2+}. This phenotype of mutants suggests that these two novel, putative ATPases may be involved in Mn^{2+} detoxification system of *M. smegmatis*. On the contrary, the complemented strains of CtpE and CtpF were not able to recover the phenotypes of these mutants. This may be due to the weakness of the mycobacterial optimal promoter that is used. Furthermore, we observed that alkali pH or Mn^{2+} did not change the expression levels of *ctpE* and *ctpF*.

We successfully cloned *ctpE* and *ctpF* from *M. smegmatis* and *M. tuberculosis* into protein expression vectors, pBAD and pEXP5-NT TOPO. After a series of protein expression and purification optimization process, CtpE was obtained in the optimal yield and purity. Therefore, we tested CtpE's phosphatase activity under various conditions; however, it did not show any activity. Although CtpF was expressed well in *E. coli,* it degraded during the purification; thus it could not be used for further analysis.

5 REFERENCES

1. Møller, J. V., Juul, B., and le Maire, M. (1996) Structural organization, ion transport, and energy transduction of P-type ATPases., *Biochim Biophys Acta 1286*, 1-51.
2. Agranoff, D., and Krishna, S. (2004) Metal ion transport and regulation in Mycobacterium tuberculosis, *Frontiers in Bioscience 9*, 2996-3006.
3. da Silva, J. J. R. F., and Williams, R. J. P. (2001) *The biological chemistry of the elements: the inorganic chemistry of life*, Oxford University Press.
4. Fraga, C. G. (2005) Relevance, essentiality and toxicity of trace elements in human health, *Molecular Aspects of Medicine 26*, 235-244.
5. Valko, M., Morris, H., and Cronin, M. T. D. Metals, Toxicity and Oxidative Stress, *Current Medicinal Chemistry 12*, 1161-1208.
6. Argüello, J. M., González-Guerrero, M., and Raimunda, D. (2011) Bacterial transition metal P(1B)-ATPases: transport mechanism and roles in virulence, *Biochemistry 50*, 9940-9949.
7. Wagner, D. (2005) Elemental analysis of Mycobacterium avium-, Mycobacterium tuberculosis-, and Mycobacterium smegmatis-containing phagosomes indicates pathogen-induced microenvironments within the host cell's endosomal system, *The Journal of immunology (1950) 174*, 1491.
8. Soldati, T. (2012) Mycobacteria and the Intraphagosomal Environment: Take It With a Pinch of Salt(s)! Sensing and Regulation of the Intraphagosomal Environment, *Traffic (Copenhagen, Denmark) 13*, 1042-1052.
9. Parham, and Peter (2009) *The	Immune	System* 3rd ed., Garland Science Publishing New York.
10. Papp-Wallace, K. M., and Maguire, M. E. (2006) Manganese Transport and the Role of Manganese in Virulence, *Annu. Rev. Microbiol. 60*, 187-209.
11. Kehres, D. G., and Maguire, M. E. (2003) Emerging themes in manganese transport, biochemistry and pathogenesis in bacteria, *Fems Microbiology Reviews 27*, 263-290.
12. Anjem, A. a. V. (2009) Manganese import is a key element of the OxyR response to hydrogen peroxide in Escherichia coli, *Mol Microbiol 72*, 844-858.
13. Rosch, J. W., Gao, G., Ridout, G., Wang, Y.-D., and Tuomanen, E. I. (2009) Role of the manganese efflux system mntE for signalling and pathogenesis in Streptococcus pneumoniae, *Molecular Microbiology 72*, 12-25.
14. Padilla-Benavides, T. (2013) A novel P1B-type Mn2 transporting ATPase is required for secreted protein metallation in mycobacteria, *The Journal of biological chemistry*.

15. Hao, Z., Chen, S., and Wilson, D. B. (1999) Cloning, expression, and characterization of cadmium and manganese uptake genes from Lactobacillus plantarum, *Appl Environ Microbiol 65*, 4746-4752.

16. Dominguez, D. C. (2004) Calcium signalling in bacteria, *Mol Microbiol 54*, 291-297.

17. Paulsen, I. T., Nguyen, L., Sliwinski, M. K., Rabus, R., and Saier Jr, M. H. (2000) Microbial genome analyses: comparative transport capabilities in eighteen prokaryotes, *Journal of Molecular Biology 301*, 75-100.

18. Waditee, R., Hossain, G. S., Tanaka, Y., Nakamura, T., Shikata, M., Takano, J., Takabe, T., and Takabe, T. (2004) Isolation and Functional Characterization of Ca2+/H+ Antiporters from Cyanobacteria, *Journal of Biological Chemistry 279*, 4330-4338.

19. Raeymaekers, L., Wuytack, E. Y., Willems, I., Michiels, C. W., and Wuytack, F. (2002) Expression of a P-type Ca2+-transport ATPase in Bacillus subtilis during sporulation, *Cell Calcium 32*, 93-103.

20. Ren, D., Navarro, B., Xu, H., Yue, L., Shi, Q., and Clapham, D. E. (2001) A Prokaryotic Voltage-Gated Sodium Channel, *Science 294*, 2372-2375.

21. Malik, Z. A. (2000) Inhibition of Ca2 signaling by Mycobacterium tuberculosisis associated with reduced phagosome–lysosome fusion and increased survival within human macrophages, *The Journal of experimental medicine 191*, 287.

22. Malik, Z. A., Iyer, S. S., and Kusner, D. J. (2001) Mycobacterium tuberculosis phagosomes exhibit altered calmodulin-dependent signal transduction: Contribution to inhibition of phagosome-lysosome fusion and intracellular survival in human macrophages, *Journal of Immunology 166*, 3392-3401.

23. Padan, E. (2005) Alkaline pH homeostasis in bacteria: New insights, *Biochimica et biophysica acta. Biomembranes 1717*, 67-88.

24. Booth, I. R. (2007) The Regulation of Intracellular pH in Bacteria, In *Novartis Foundation Symposium 221 - Bacterial Responses to pH*, pp 19-37, John Wiley & Sons, Ltd.

25. Iivanainen, E., Martikainen, P., Vaananen, P., and Katila, M. L. (1999) Environmental factors affecting the occurrence of mycobacteria in brook sediments, *Journal of Applied Microbiology 86*, 673-681.

26. Oh, Y. K., and Straubinger, R. M. (1996) Intracellular fate of Mycobacterium avium: use of dual-label spectrofluorometry to investigate the influence of bacterial viability and opsonization on phagosomal pH and phagosome-lysosome interaction, *Infection and Immunity 64*, 319-325.

27. Sturgill-Koszycki, S., Schlesinger, P. H., Chakraborty, P., Haddix, P. L., Collins, H. L., Fok, A. K., Allen, R. D., Gluck, S. L., Heuser, J., and Russell, D. G. (1994) Lack of acidification in Mycobacterium phagosomes produced by exclusion of the vesicular proton-ATPase, *Science 263*, 678-681.

28. Rao, M., Streur, T. L., Aldwell, F. E., and Cook, G. M. (2001) Intracellular pH regulation by Mycobacterium smegmatis and Mycobacterium bovis BCG, *Microbiology 147*, 1017-1024.

29. O'Brien, L. M. (1996) Response of to acid stress, *FEMS microbiology letters 139*, 11-17.

30. Clemens, D. L., and Horwitz, M. A. (1995) Characterization of the mycobacterium-tuberculosis phagosome and evidence that phagosomal maturation is inhibited, *Journal of Experimental Medicine 181*, 257-270.

31. Flynn, J. L., and Chan, J. (2001) Immunology of tuberculosis., *Annu Rev Immunol 19*, 93-129.

32. Clark-Curtiss, J. E. (2003) M G P, *Annual review of microbiology 57*, 517-549.

33. Rengarajan, J., Bloom, B. R., and Rubin, E. J. (2005) Genome-wide requirements for Mycobacterium tuberculosis adaptation and survival in macrophages., *Proc Natl Acad Sci U S A 102*, 8327-8332.

34. Tottey, S., Waldron, K. J., Firbank, S. J., Reale, B., Bessant, C., Sato, K., Cheek, T. R., Gray, J., Banfield, M. J., Dennison, C., and Robinson, N. J. (2008) Protein-folding location can regulate manganese-binding versus copper- or zinc-binding, *Nature 455*, 1138-1142.

35. Waldron, K. J., and Robinson, N. J. (2009) How do bacterial cells ensure that metalloproteins get the correct metal?, *Nat Rev Micro 7*, 25-35.

36. Nies, D. H. (2003) Efflux-mediated heavy metal resistance in prokaryotes, *FEMS Microbiology Reviews 27*, 313-339.

37. Ma, Z. (2009) Coordination Chemistry of Bacterial Metal Transport and Sensing, *Chemical reviews 109*, 4644-4681.

38. Skou, J. C. (1957) The influence of some cations on an adenosine triphosphatase from peripheral nerves, *Biochimica et biophysica acta 23*, 394-401.

39. Axelsen, K. B., and Palmgren, M. G. (1998) Evolution of Substrate Specificities in the P-Type ATPase Superfamily, *Journal of Molecular Evolution 46*, 84-101.

40. Lutsenko, S., and Kaplan, J. H. (1995) Organization of P-type ATPases: significance of structural diversity, *Biochemistry 34*, 15607-15613.

41. Axelsen, K. B., and Palmgren, M. G. (2001) Inventory of the Superfamily of P-Type Ion Pumps in Arabidopsis, *Plant Physiology 126*, 696-706.

42. Kuhlbrandt, W. (2004) Biology, structure and mechanism of P-type ATPases, *Nat Rev Mol Cell Biol 5*, 282-295.

43. Stokes, D. L., and Green, N. M. (2003) Structure and function of the calcium pump., *Annu Rev Biophys Biomol Struct 32*, 445-468.

44. Mandal, D., Rulli, S. J., and Rao, R. (2003) Packing Interactions between Transmembrane Helices Alter Ion Selectivity of the Yeast Golgi Ca2+/Mn2+-ATPase PMR1, *Journal of Biological Chemistry 278*, 35292-35298.

45. Jorgensen, P. L., Hakansson, K. O., and Karlish, S. J. (2003) Structure and mechanism of Na,K-ATPase: functional sites and their interactions., *Annu Rev Physiol 65*, 817-849.

46. Eraso, P., and Gancedo, C. (1987) Activation of yeast plasma membrane ATPase by acid pH during growth., *FEBS Lett 224*, 187-192.

47.   Post, R. L. (1965) AN ENZYMATIC MECHANISM OF ACTIVE SODIUM AND POTASSIUM TRANSPORT, *The journal of histochemistry and cytochemistry 13*, 105-112.

48.   Niggli, V. (2008) Anticipating antiport in P-type ATPases, *Trends in biochemical sciences (Amsterdam. Regular ed.) 33*, 156-160.

49.   Agranoff, D. D., and Krishna, S. (1998) Metal ion homeostasis and intracellular parasitism, *Molecular Microbiology 28*, 403-412.

50.   Chan, H., Babayan, V., Blyumin, E., Gandhi, C., Hak, K., Harake, D., Kumar, K., Lee, P., Li, T. T., Liu, H. Y., Lo, T. C., Meyer, C. J., Stanford, S., Zamora, K. S., and Saier, M. H. (2010) The p-type ATPase superfamily., *J Mol Microbiol Biotechnol 19*, 5-104.

51.   Botella, H., Stadthagen, G., Lugo-Villarino, G., de Chastellier, C., and Neyrolles, O. (2012) Metallobiology of host-pathogen interactions: an intoxicating new insight, *Trends in Microbiology 20*, 106-112.

52.   Cole, S. T., Brosch, R., Parkhill, J., Garnier, T., Churcher, C., Harris, D., Gordon, S. V., Eiglmeier, K., Gas, S., Barry, C. E., Tekaia, F., Badcock, K., Basham, D., Brown, D., Chillingworth, T., Connor, R., Davies, R., Devlin, K., Feltwell, T., Gentles, S., Hamlin, N., Holroyd, S., Hornsby, T., Jagels, K., Krogh, A., McLean, J., Moule, S., Murphy, L., Oliver, K., Osborne, J., Quail, M. A., Rajandream, M. A., Rogers, J., Rutter, S., Seeger, K., Skelton, J., Squares, R., Squares, S., Sulston, J. E., Taylor, K., Whitehead, S., and Barrell, B. G. (1998) Deciphering the biology of Mycobacterium tuberculosis from the complete genome sequence, *Nature 393*, 537-544.

53.   Ward, S. K. (2010) CtpV: a putative copper exporter required for full virulence of Mycobacterium tuberculosis Copper transport and virulence in Mycobacterium tuberculosis, *Molecular microbiology 77*, 1096-1110.

54.   Botella, H., Peyron, P., Levillain, F., Poincloux, R., Poquet, Y., Brandli, I., Wang, C., Tailleux, L., Tilleul, S., Charrière, G. M., Waddell, Simon J., Foti, M., Lugo-Villarino, G., Gao, Q., Maridonneau-Parini, I., Butcher, Philip D., Castagnoli, Paola R., Gicquel, B., de Chastellier, C., and Neyrolles, O. (2011) Mycobacterial P1-Type ATPases Mediate Resistance to Zinc Poisoning in Human Macrophages, *Cell Host & Microbe 10*, 248-259.

55.   Raimunda, D., Long, J. E., Sassetti, C. M., and Argüello, J. M. (2012) Role in metal homeostasis of CtpD, a Co^{2+} transporting P(1B4)-ATPase of Mycobacterium smegmatis, *Mol Microbiol 84*, 1139-1149.

56.   Sassetti, C. M. (2003) Genetic requirements for mycobacterial survival during infection, *National Academy of Sciences 100*, 12989.

57.   Cole, S. T., Eiglmeier, K., Parkhill, J., James, K. D., Thomson, N. R., Wheeler, P. R., Honoré, N., Garnier, T., Churcher, C., Harris, D., Mungall, K., Basham, D., Brown, D., Chillingworth, T., Connor, R., Davies, R. M., Devlin, K., Duthoy, S., Feltwell, T., Fraser, A., Hamlin, N., Holroyd, S., Hornsby, T., Jagels, K., Lacroix, C., Maclean, J., Moule, S., Murphy, L., Oliver, K., Quail, M. A., Rajandream, M. A., Rutherford, K. M., Rutter, S., Seeger, K., Simon, S., Simmonds, M., Skelton, J., Squares, R., Squares,

S., Stevens, K., Taylor, K., Whitehead, S., Woodward, J. R., and Barrell, B. G. (2001) Massive gene decay in the leprosy bacillus., *Nature 409*, 1007-1011.

58. van Kessel, J. C. (2007) Recombineering in Mycobacterium tuberculosis, *Nature methods 4*, 147-152.

59. Studier, F. W. (2005) Protein production by auto-induction in high-density shaking cultures, *Protein Expression and Purification 41*, 207-234.

60. Mandal, A. K., Cheung, W. D., and Arguello, J. M. (2002) Characterization of a thermophilic P-type Ag+/Cu+-ATPase from the extremophile Archaeoglobus fulgidus, *Journal of Biological Chemistry 277*, 7201-7208.

61. Bradford, M. M. (1976) A rapid and sensitive method for the quantitation of microgram quantities of protein utilizing the principle of protein-dye binding, *Anal Biochem 72*, 248-254.

62. Yang, Y., Mandal, A. K., Bredeston, L. M., González-Flecha, F. L., and Argüello, J. M. (2007) Activation of Archaeoglobus fulgidus Cu(+)-ATPase CopA by cysteine, *Biochim Biophys Acta 1768*, 495-501.

63. Edgar, R. C. (2004) MUSCLE: multiple sequence alignment with high accuracy and high throughput, *Nucleic acids research 32*, 1792-1797.

64. Gouet, P. (1999) ESPript: analysis of multiple sequence alignments in PostScript, *Bioinformatics (Oxford, England) 15*, 305-308.

65. Krogh, A. (2001) Predicting transmembrane protein topology with a hidden markov model: application to complete genomes, *Journal of molecular biology 305*, 567-580.

66. Seeliger, D. (2010) Ligand docking and binding site analysis with PyMOL and Autodock/Vina, *Journal of computer-aided molecular design 24*, 417-422.

67. Sørensen, T. L.-M., Clausen, J. D., Jensen, A.-M. L., Vilsen, B., Møller, J. V., Andersen, J. P., and Nissen, P. (2004) Localization of a K+-binding Site Involved in Dephosphorylation of the Sarcoplasmic Reticulum Ca2+-ATPase, *Journal of Biological Chemistry 279*, 46355-46358.

68. Sorensen, T. L. M. (2004) Phosphoryl Transfer and Calcium Ion Occlusion in the Calcium Pump, *Science (New York, N.Y.) 304*, 1672-1675.

69. Faxen, K. (2011) Characterization of a Listeria monocytogenes Ca2 Pump: A SERCA-TYPE ATPase WITH ONLY ONE Ca2 -BINDING SITE, *The Journal of biological chemistry 286*, 1609-1617.

70. Guinn, K. M. (2004) Individual RD1-region genes are required for export of ESAT-6/CFP-10 and for virulence of Mycobacterium tuberculosis RD1 genes affect secretion and virulence of M. tuberculosis, *Molecular microbiology 51*, 359-370.

APPENDIX. Primers used for PCR amplifications

Primer Name	Recognition Sequence
qCtpE-MSM_Forward	ATCGTGCTGCTGGACAACAAGTT
qCtpE- MSM_Reverse	AGTACACGGTCTTGGTGAGGAAC
qCtpF- MSM_Forward	CTCGGCATGTTTCTCTGGGAGTT
qCtpF- MSM_Reverse	AGGTTCGAGGAGGAAGCGATTGT
Msmeg_CtpE_HpaI	GATCAAGTTAACATGACGACGAT
Msm_CtpE_KpnI	GATCATGGTACCCTATCTCCACACGCGCCGTTCTTC
Msmeg_CtpF_HpaI	GTAATGTTAACGTGCGACGGCCG
Msm_CtpF_KpnI	GTAATGGTACCCTACCGATGGGCGGCGGTGTG
Mtb_CtpE_HpaI	GGAGCAGTTAACATGACCCGTTC
Mtb_CtpE_KpnI	GCATATGGTACCTTATCGCCACACTCTCGGTTTCAC
Mtb_CtpF_HpaI	GCGGAGTTAACTTGTCGGCGTCA
Mtb_CtpF_ KpnI	GCATATGGTACCTCATGGCGGTTGCGCCCGTATTC
CtpG_AccII FWD	GCATAACGTTGTGACGACTGTAGTTGACGCCGAG
CtpG_XbaI RVS	GCAATCTAGACTACCCCGGGATAGTCCGATCAGG
3'CtpE Mtb H37Rv	TCGCCACACATCTCGGTTTCAC
5'CtpE Mtb H37Rv	ACCCGTTCGGCTTCGGCG
Msmeg 5636 FWD	ATGACGACGATGGCTGCCGCCGGCCTCACC
Msmeg_5636_TEV RVS	GGATCGAAAATACAGGTTTTCGCCGCTGCTTCTCCACACGCGCCGTTC
CtpG 5'UTR_F	GATGCGGCCGCCTTGGGCGAGTTGGTCCAGGTC
CtpG 5'UTR_R	GGCCACTAGTCGGCCCGTCCCGCGTCGAACTG
CtpG 3'UTR_F	GGCCCTCGAGGCGGTCGTGCTTGTGCACGAG

CtpG 3'UTR_R	GATTGGGCCCGACTGCCTGATGGCGGCCCG
MtbCtpE 5'UTR_F	GATTGCGGCCGCGAGACGCTGACCGCCGAATTC
MtbCtpE 5'UTR_R	GGCCACTAGTCGATCTGCCCGACGGTGCGGGTG
MtbCtpE 3'UTR_F	GATCCTCGAGACGACGTCAATCGCGCTGGCGG
MtbCtpE 3'UTR_R	CATTGGGCCTCGTCGCTGCCCAGCCTGAGG
MtbCtpF 5'UTR_F	GATTGCGGCCGCTGCACAAAGTCGTGGTGTGCGAT
MtbCtpF 5'UTR_R	GGACACTAGTGGGCGGCCTCGCCGTCGGACAGC
MtbCtpF 3'UTR_F	GGCCCTCGAGGCGCCAATCGATATCGGGGTGTG
MtbCtpF 3'UTR_R	CATTGGGCCCGCCGATACCACCAGGCACGATCCAG